Extreme weather events modulate processing and export of dissolved organic carbon in the Neuse River Estuary, NC

Alexandria G. Hounshell[a,*], Jacob C. Rudolph[b], Bryce R. Van Dam[c], Nathan S. Hall[a], Christopher L. Osburn[b], Hans W. Paerl[a]

[a] Institute of Marine Sciences, University of North Carolina – Chapel Hill, 3431 Arendell St, Morehead City, NC, 28557, United States
[b] Department of Marine, Earth, and Atmospheric Sciences, North Carolina State University, 2800 Faucette Dr., Raleigh, NC, 27695, United States
[c] Department of Biological Sciences, Florida International University, 11200 SW 8th St, Miami, FL, 33199, United States

ARTICLE INFO

Keywords:
Dissolved organic carbon
Colored dissolved organic matter
Extreme weather events
USA
North Carolina
Neuse River Estuary

ABSTRACT

As the interface between riverine and coastal systems, estuaries play a key role in receiving, transporting, and processing terrestrial organic carbon prior to export to downstream coastal systems. Estuaries can switch from terrestrial organic carbon reactors under low river flow to pipelines under high flow, but it remains unclear how estuarine terrestrial organic carbon processing responds to the full spectrum of discharge conditions, which are bracketed by these high and low discharge events. The amount of terrestrial dissolved organic carbon and colored dissolved organic matter imported, processed, and exported was assessed for riverine discharge events spanning from the 4th to 99th flow quantiles in the Neuse River Estuary, North Carolina, USA using spatially and temporally (July 2015–December 2016) resolved measurements. The extent of dissolved organic matter processing in the estuary under various flow conditions was estimated using a non-steady state box model to calculate estuary-wide terrestrial dissolved organic carbon and colored dissolved organic matter source & sink terms. Under mid-range riverine discharge conditions (4th to 89th flow quantiles), the Neuse River Estuary was a sink for terrestrial dissolved organic carbon, retaining and/or processing (i.e., flocculation; photochemical and microbial degradation) on average ~29% of terrestrial dissolved organic carbon. Following floods due to extreme precipitation events (99th flow quantile), however, over 99% of the terrestrial dissolved organic carbon loaded from the riverine end-member was exported directly to the downstream coastal system. Following such extreme weather events, the estuary acts as a pipeline for direct export of terrestrial dissolved organic carbon, drastically altering the amount and quality of dissolved organic carbon loaded to downstream coastal systems. This has important implications under future climate scenarios, where extreme weather events are expected to increase.

1. Introduction

The past two decades have witnessed an increased focus on the function, transport, cycling, and storage of dissolved organic carbon (DOC) from headwater streams to the coastal ocean (Bauer et al., 2013; Bianchi, 2011). Much of this research has centered on the transport of terrestrial DOC (tDOC) from soils to streams, specifically how the quantity and quality of tDOC in streams change in response to factors like: discharge, antecedent soil wetness, temperature, and seasonality (Dhillon and Inamdar, 2013; Raymond and Saiers, 2010; Sanderman et al., 2009; Yoon and Raymond, 2012). It is well documented that extreme weather events (EWEs) defined here as river flow ≥ 99th flow quantile, including tropical storms and hurricanes, magnify precipitation and discharge in streams and rivers, resulting in increased fluxes of tDOC in downstream aquatic systems (Bauer et al., 2013; Raymond et al., 2016; Raymond and Saiers, 2010), including coastal rivers and estuaries (Bianchi et al., 2013; Osburn et al., 2012; Paerl et al., 2018).

During EWEs, there is a 'pulse' of tDOC exported from land to adjacent streams and rivers, as conceptualized by the pulse-shunt concept (PSC) (Raymond et al., 2016). This tDOC pulse is then 'shunted' and transported further downstream than would typically occur under baseflow conditions. The pulse-shunt mechanism results in the upper stream and river systems acting as a pipeline for the transport of tDOC to downstream ecosystems. While the PSC has been applied to headwater streams and rivers, it has yet to be applied to downstream, estuarine systems. Previous studies examining the impact of tropical cyclone events on estuaries show that under these conditions, minimal amounts of the tDOC received by estuaries is processed, leading to

* Corresponding author.
E-mail address: alexgh@live.unc.edu (A.G. Hounshell).

https://doi.org/10.1016/j.ecss.2019.01.020
Received 8 October 2018; Received in revised form 13 January 2019; Accepted 25 January 2019
Available online 04 February 2019

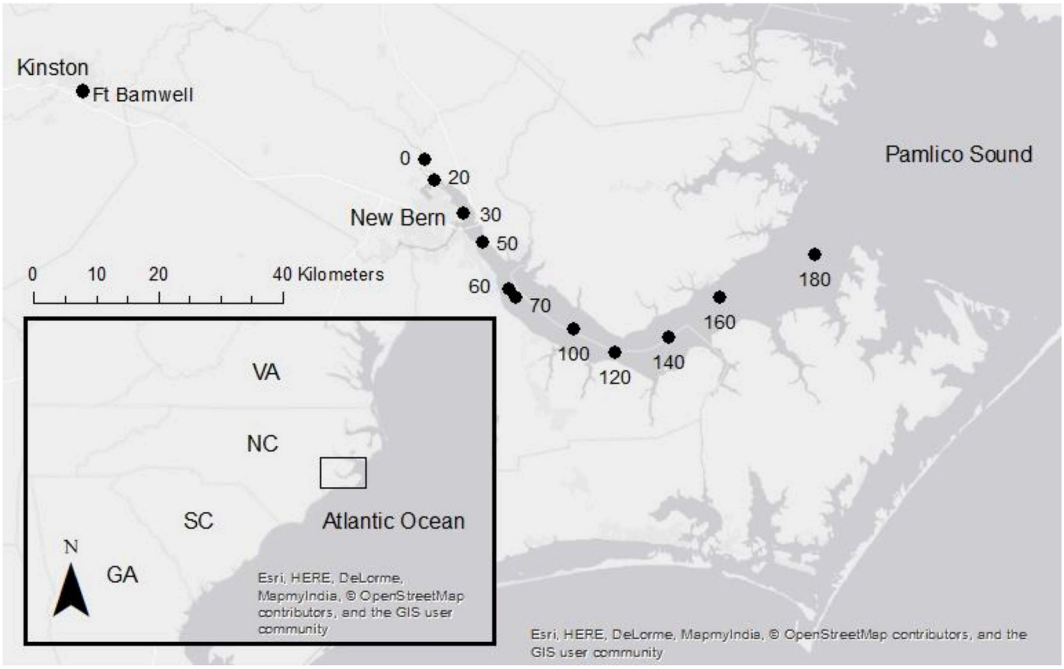

Fig. 1. Map of the NRE located in Eastern NC. ModMon sampling stations start at Station 0 at the head of the estuary to Station 180 at the mouth of the estuary. Ft. Barnwell is the location of the USGS gaging station used for riverine discharge.

subsequent export of tDOC to coastal waters (Bauer et al., 2013; Bianchi et al., 2013).

Under baseflow conditions when flushing times are relatively long, estuaries are thought to be sites of tDOC processing prior to export to the coastal ocean (Del Giorgio and Pace, 2008). Processing of tDOC includes its conversion to dissolved inorganic C (DIC) via microbial and photochemical degradation, which may push estuaries towards net CO_2 emission (Bauer et al., 2013; Bianchi et al., 2013; Crosswell et al., 2014, 2012; Van Dam et al., 2018). The role estuaries play, as either reactors or conduits for tDOC under varying discharge conditions, has important implications for understanding their function as sites of tDOC consumption and DIC production prior to export to the coastal ocean. This is especially important in the larger context of climate change, where the frequency and intensity of EWEs are predicted to increase, including along the US east coast (Bender et al., 2009; Janssen et al., 2016).

While several studies have assessed the binary impact of variable river discharge, as either baseflow or extreme-flow, on tDOC in estuaries (Bianchi et al., 2013; Dixon et al., 2014; Osburn et al., 2012; Paerl et al., 2006, 2001), few studies have evaluated the full continuum of flow conditions, from baseflow to extreme-flow. Prior studies conducted in the Neuse River Estuary (NRE), North Carolina indicate that, under low-flow conditions, physical factors like river discharge, wind speed and wind direction are dominant controls on estuarine dissolved organic matter (DOM) quantity and quality (Dixon et al., 2014). Following tropical cyclone events, associated with elevated precipitation and river discharge, studies conducted in this system have demonstrated tDOC enrichment from elevated river inputs throughout the estuary and adjacent sound, including after Hurricane Fran in 1996 (Paerl et al., 1998), Hurricanes Dennis, Floyd and Irene in 1999 (Paerl et al., 2001, 2006), and Hurricane Irene in 2011 (Osburn et al., 2012). The 1999 hurricane season resulted in organic matter (OM) inputs which led to long-term internal nutrient loading to the NRE (Paerl et al., 2006), indicating that tropical cyclone events and associated precipitation and river discharge can have long-term impacts on coastal lagoons due to their long flushing times (Peierls et al., 2003).

More recent studies in the NRE assessing the impact of Hurricane Irene in September 2011 also demonstrated an increase in tDOC following this event and observed changes in DOM and particulate OM (POM) quality from that produced by phytoplankton to more terrestrial OM sources (Osburn et al., 2012). The large CO_2 efflux out of the NRE observed during and immediately following (~1 day) Hurricane Irene, was partially attributed to conversion of re-suspended sedimentary OC to DIC. However, in the ~2 weeks following this event, the sustained CO_2 efflux was attributed to increased rates of biological and photochemical tDOC processing, loaded into the system during the storm (Crosswell et al., 2014). While tDOC processing and air-water CO_2 exchange in estuaries may represent significant fluxes in the global C cycle, quantitative links between these processes have yet to be clarified, especially after EWEs.

The goal of this study was to examine the response of DOC quantity and quality to a range of flow conditions spanning from baseflow to a 99th flow quantile event in a shallow, microtidal estuary, the NRE, by analyzing seven discrete discharge events captured from July 20, 2015 to December 13, 2016. We hypothesized that large-scale changes in tDOC dynamics of the NRE following EWEs indicate the system may be able to move from a simple "pipeline" of tDOC export immediately following an event to a reactor in the weeks (~2–3 weeks) following these events as the system returns to normal flow conditions.

2. Methods

2.1. Study site and sampling methods

The NRE is a shallow (average depth ~3.5 m), micro-tidal (< 4 cm tidal range) estuary located in the coastal plain of NC (Luettich et al., 2002) (Fig. 1). The NRE watershed extends from the urbanized Raleigh-Durham metropolitan area through rural eastern NC, where land use is mainly characterized as agricultural (row crop; concentrated animal feeding operations), forested, and freshwater wetlands (Rothenberger et al., 2009; Stow et al., 2001). The NRE extends from Streets Ferry Bridge (station 0), north of New Bern, NC to the outlet into Pamlico Sound (PS) (station 180) (Fig. 1). Combined, the NRE-PS is the USA's largest lagoonal estuarine complex. It is bounded to the east by the Outer Banks barrier islands which limit exchange between NRE-PS and W. Atlantic ocean waters, leading to long flushing times in the NRE (average ~ 5–8 weeks) (Peierls et al., 2012). This allows sufficient time for consumption of inorganic nutrients and degradation of OM in the estuary (Christian et al., 1991; Paerl et al., 1998).

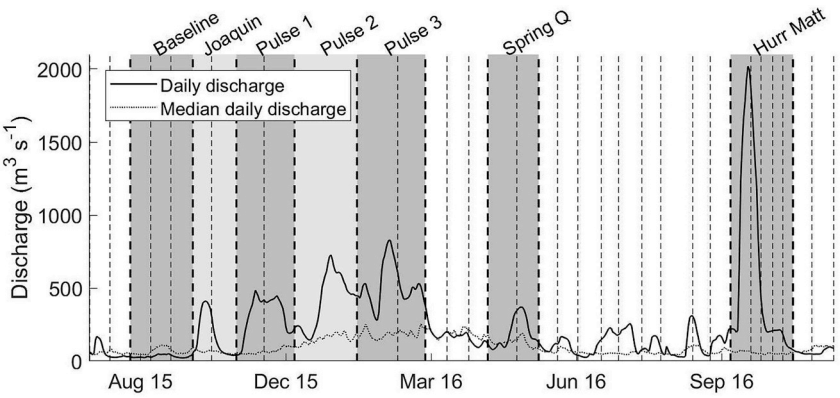

Fig. 2. Daily discharge (black lines) obtained from Ft. Barnwell USGS gaging station plotted for the study period. The grey dashed line corresponds to the median daily discharge from 1997 to 2017. Dashed vertical lines correspond to ModMon sampling dates. Bolded dashed vertical lines are bounds for each discrete discharge event (1–7) (Table 1).

The NRE has been the site of extensive water quality monitoring assessments (1994 - present) conducted by the University of North Carolina – Chapel Hill (UNC−CH), Institute of Marine Sciences (IMS), Neuse River Monitoring and Modeling project (ModMon; http://paerllab.web.unc.edu/projects/modmon/) (Luettich et al., 2000). We used ModMon data for the NRE from July 20, 2015 to December 13, 2016. Water quality assessments including DOC, colored DOM (CDOM), and primary production (PP) were conducted on samples collected from the middle channel of the NRE at 11 stations across the estuary (SI, Table S2), from the location of maximum salinity intrusion (station 0) to the estuary mouth near PS (station 180) (Fig. 1). Assessments from July 20, 2015 to October 3, 2016 were conducted twice-monthly from March to October and monthly from November to February. Assessments from October 17, 2016 to December 13, 2016 were conducted weekly as part of a project to assess the impacts of Hurricane Matthew (October 7–8, 2016) on PP and water quality in the NRE following this extreme flood event (Musser et al., 2017).

At each sampling station and time point salinity was measured from surface (0.2 m below surface) to bottom (0.5 m above bottom) at 0.5 m intervals using a YSI 6600 multi-parameter, water quality sonde (Hall et al., 2013). Surface (0.2 m below surface) and bottom (0.5 m above bottom) water samples were collected for various chemical analyses at each of the 11 stations. Samples were maintained in the dark at ambient temperature and returned to UNC-CH IMS located in Morehead City, NC within ~6 h of collection then filtered through a combusted (450 °C, 4 h) 0.7 μm mesh size, GF/F glass fiber filter. The filtrate was collected and frozen at −20 °C in the dark until DOM quantitative and qualitative analyses.

DOC concentration ([DOC]) was determined via high-temperature catalytic oxidation, using a Shimadzu TOC-5000 analyzer (Peierls et al., 2003). CDOM absorbance was measured on samples collected from July 20, 2015 to July 18, 2016 and from October 3, 2016 to December 13, 2016. UNC-CH IMS measured absorbance on samples collected prior to Hurricane Matthew (July 2015–July 2016; October 3, 2016). Absorbance spectra (200–800 nm) on filtered surface samples were measured on a Shimadzu UV-1700 Pharma-Spec spectrophotometer. For samples following Hurricane Matthew (October 17, 2016 to December 13, 2016), absorbance spectra were determined by the Osburn Laboratory at North Carolina State University (NCSU) on a Varian Cary 300UV spectrophotometer. Absorbance spectra were corrected using a Nanopure (UNC−CH IMS) or Milli-Q (NCSU) water blank collected on the same day as analysis. All samples with > 0.4 raw absorbance units at 240 nm were diluted (Osburn et al., 2012). Absorbance values at 350 nm were converted to Naperian absorbance coefficients (a_λ, m^{-1}) (Spencer et al., 2013). A comparison between UNC-CH IMS and NCSU measured absorbance values at 350 nm (a_{350}) is presented in the SI, Appendix 1 (n = 6) (Table S1). NCSU values were on average, 11% greater than values measured at UNC-CH IMS.

Neuse River (NR) freshwater discharge data were collected from USGS gauging station #02091814 located at Ft. Barnwell, NC about 26 km upstream of station 0 (Paerl et al., 2014). To account for freshwater inputs downstream of the gauging station, discharge data from Ft. Barnwell was scaled to the area of the un-gaged watershed (31% un-gaged watershed) (Peierls et al., 2012).

2.2. DOM load

To assess changes in DOC quantity and quality related to specific discharge events, the sampling period was divided into seven discrete segments. Each event corresponded to a ~40 day time span (range: 29–44 days; mean = 38 days; median = 41 days) between ModMon sampling dates with each time span starting prior to the defined discharge event and spanning the rising and falling limb of the hydrograph (Fig. 2; Table 1). A baseline period was designated at the beginning of sampling which corresponded to a period of below median discharge (< 67 $m^3 s^{-1}$). This was followed by an increase in discharge during September–October 2015 associated with bands of Hurricane Joaquin and its associated Nor'easter. Joaquin was followed by a winter period of above average discharge, which was divided into three distinct events termed: Pulse 1, Pulse 2, and Pulse 3. In the spring of 2016, there was a distinct discharge event in the NRE which was designated as Spring Q. Finally, in fall 2016 Hurricane Matthew delivered extreme amounts of rainfall over the study area and its watershed, resulting in record discharge measured at Ft. Barnwell.

The freshwater flushing time for station 160 was calculated using the date-specific fraction of freshwater method (Alber and Sheldon, 1999) as described in Peierls et al. (2012). The date-specific average discharge is an iterative calculation that averages the riverine discharge over the flushing time period. This allows for the most accurate calculation of the freshwater flushing time in an estuary experiencing highly variable discharge conditions (Alber and Sheldon, 1999).

For each discrete discharge event and the entire sampling period, DOC and a_{350} loads at station 0 were calculated using weighted regressions on time, discharge and season (WRTDS) (Stackpoole et al., 2017). WRTDS fits a relationship between continuous discharge (Q) and discrete measurements of [DOC] and a_{350} to model DOC and a_{350} riverine concentration accounting for variation in discharge, season, and time using the following equation:

$$\ln(c) = \beta_1 + \beta_2(\ln(Q)) + \beta_3(T) + \beta_4 \sin(2\pi T) + \beta_5 \cos(2\pi T) + \varepsilon \quad (1)$$

where c is the concentration, Q is the measured discharge, T is time in decimal years, ε is the error, and β_1-β_5 are the coefficients estimated from the sample data. [DOC] and a_{350} were calculated by WRTDS using the EGRET R-package (Hirsch and De Cicco, 2015; https://CRAN.R-project.org/package=EGRET). By coupling continuous discharge (Q) measurements at Ft. Barnwell with measurements of [DOC] and a_{350} collected discretely at Station 0, it is possible to interpolate the total DOC and a_{350} load to the estuary, using the WRTDS concentration estimates, over the entire time period (July 20, 2015–December 13, 2016) and across each discrete discharge event.

There is some uncertainty associated with these load estimates, particularly as the discharge and [DOC] and a_{350} measurements were

Table 1
Discharge values for the seven discrete discharge events. Historical data were calculated from median discharge values from 1997 to 2017. Cumulative discharge refers to the averaged daily discharge ($m^3\ s^{-1}$) summed over the corresponding time period.

Time Period	Description	Dates	Number of days	Average Q ($m^3\ s^{-1}$)	Average of historical median Q ($m^3\ s^{-1}$)	Cumulative Q (m^3)	Historical cumulative Q (m^3)
	All	07/20/15–12/13/16	513	237	98	120,321	50,046
1	Baseline	08/17/15–09/29/15	44	32	67	1425	2965
2	Joaquin	09/29/15–10/29/15	31	143	63	3994	1942
3	Pulse #1	10/29/15–12/08/15	41	312	69	12,805	2812
4	Pulse #2	12/08/15–01/20/16	44	411	151	17,661	6652
5	Pulse #3	01/20/16–03/07/16	48	517	188	24,810	9015
6	Spring Q	04/19/16–05/24/16	36	192	129	6904	4655
7	Hurricane Matthew	10/03/16–11/15/16	44	625	56	27,518	2486

collected at two different locations. The greatest uncertainty is associated with the discharge measurements, as these values were measured 26 km upstream from the head of the estuary. However, there are no large tributaries to the NR between Ft. Barnwell and the head of the estuary (Station 0). Additionally, the discharge measured at Ft. Barnwell was scaled to the area of un-gaged watershed to account for any additional tributaries (Peierls et al., 2012). Therefore, while we acknowledge the [DOC] and a_{350} loads are estimates, we feel confident that they accurately capture the variability and dynamics of riverine OC loading to the NRE.

2.3. Volume weighted DOM concentrations

Volume-weighted averaged salinity, [DOC] and a_{350} were calculated for each sampling date in the NRE from station 20 to 160. Briefly, the mean value for each station (as surface and bottom) was multiplied by the volume of each segment centered on the respective station, as calculated for the box models (SI Fig. S1). The product for each segment was then summed and divided by the total volume of the estuary (Peierls et al., 2012). These volume-weighted averages serve as a representation of the total DOM (as [DOC] or a_{350}) pool contained in the NRE at each ModMon sampling accounting for differences in volume in the upper versus lower estuary.

2.4. DOM source/sink term

A box model approach following Hagy et al. (2000), was used to estimate flow out of the estuary (surface flow) and into the estuary (bottom flow) at station 160 for each ModMon date (SI, Appendix 4). Briefly, the estuary was divided into nine boxes with each box centered on a ModMon sampling station (station 20–160). For each sampling date, the head of the estuary was defined as the most upstream site with measurable salinity and vertical stratification. The defined head of the estuary ranged from station 20 during low flow to station 140 following the Pulse 3 event, when discharge was consistently above the historical median. Stations upstream of the designated head of the estuary were treated as 'river boxes'. The head of the estuary was designated as a 'transition box' where the river transitions into the estuary, the first signs of salt were observed, and estuarine circulation began. Downstream of the transition box, each box was divided by the depth of the pycnocline into a surface and bottom layer to represent stratification. These boxes were designated 'estuarine boxes' and the surface discharge out of each box was calculated along with the bottom salt water influx. A more detailed description of the salinity box model can be found in the SI (Appendix 4). The 95% confidence intervals were determined for all box model calculations assuming that discharge data varied up to 14% from the measured value (Q ± 14%), [DOC] varied up to 2.3% ([DOC] ± 2.3%), and a_{350} varied 11% (a_{350} ± 11%). A discussion of uncertainty values is included in the SI (Appendix 5).

Once flows into and out of each designated box were determine using the salinity box model, it was possible to calculate a DOC ($kg\ d^{-1}$) and a_{350} ($m^2\ d^{-1}$) source & sink term for each box (SI, Appendix 4). A cumulative source & sink term was calculated for the entire estuary at each time point by summing the nine individual box source & sink terms. The respective DOM source & sink term represented any source & sink processes that occur in the estuary besides conservative mixing. A source indicates internal estuarine production of terrestrial-like DOC not accounted for in the box model (i.e., porewater resuspension; inputs from un-gaged tributaries and wetlands; production by primary and microbial production), while a sink indicates internal estuarine consumption of tDOC (i.e., microbial or photochemical oxidation and conversion to DIC; flocculation). For consistency with other parameters (i.e., CO_2 flux), the final calculated source & sink term was multiplied by −1 to ensure source terms were positive and sink terms were negative. Time points where the confidence intervals spanned zero were not plotted in subsequent graphs (DOC: 9/19/2016; a_{350}: 11/8/16, 11/

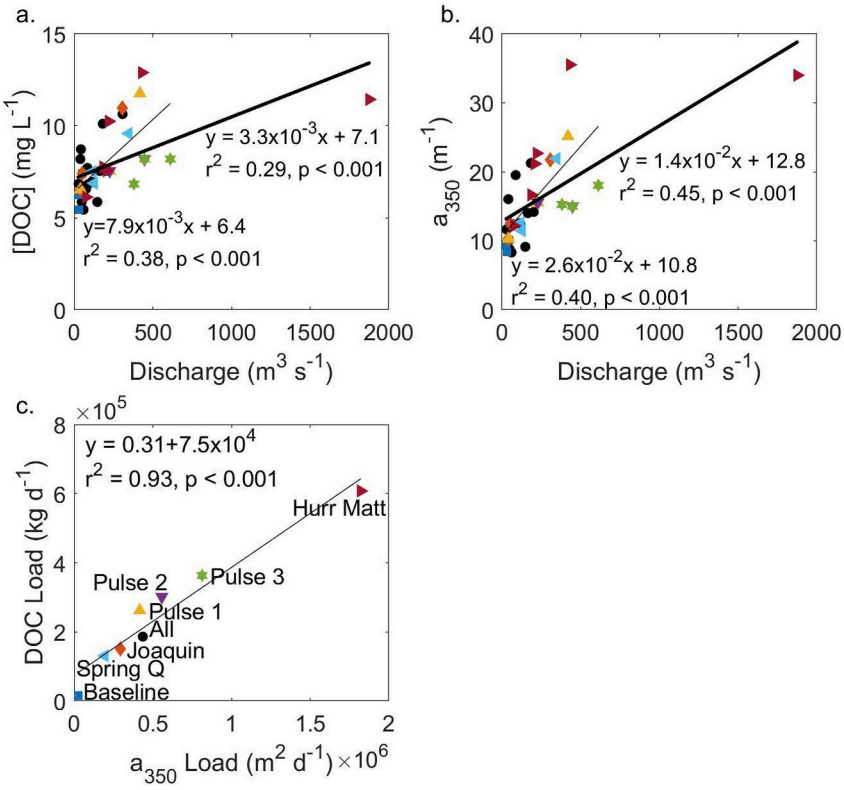

Figure 3. a. [DOC] (mg L^{-1}) and b. a_{350} (m^{-1}) plotted against discharge (m^3 s^{-1}). c. DOC load (kg d^{-1}) plotted against a_{350} load (m^2 d^{-1}). Discrete discharge events are identified by colors and symbols as indicated in Fig. 3c. A linear regression equation, coefficient of determination (r^2) and p-value from a *t*-test comparing the slope to zero are displayed on each graph (bolded line; mid-graph, right). A linear regression excluding the anomalously high discharge event occurring immediately after Hurricane Matthew is also plotted (thin line; bottom, left).

15/16). A more detailed description of the DOC and a_{350} box model can be found in the SI (Appendix 4). Associated code and datasets used for the salinity and DOC and a_{350} box models can be accessed on the projects GitHub page (DOI: https://doi.org/10.5281/zenodo.2550075).

2.5. Estimates of biological processes

CO_2 flux out of the estuary and production of DOC by PP were used to constrain the major biological sources and sinks of DOC in the NRE. Determinations of sea-to-air CO_2 flux were obtained from Van Dam et al. (2018) for July 20, 2015 to October 17, 2016. Briefly, Van Dam et al. (2018) measured in-situ, surface water partial pressure CO_2 (pCO_2) using a shower-head gas equilibrator paired with an infrared detector (LI-COR, Li-840A) along longitudinal transects from the head of the NRE (Station 30) to the outlet at PS (Station 180). The NRE was divided into upper-, mid-, and lower-estuary sections and CO_2 fluxes were calculated for each section from distance-weighted pCO_2, temperature and salinity, along with gas transfer velocities derived from daily-average wind speed (Jiang et al., 2008). The upper-, mid-, and lower-estuary CO_2 fluxes as reported by Van Dam et al. (2018) were aerially weighted to calculate the total CO_2 flux for the NRE at each time point. It is important to note these CO_2 fluxes represent the net sea-to-air CO_2 flux, and include CO_2 transported in from the river, as well as net biological and photochemical processes in the estuary.

PP was measured using the ^{14}C method on surface water samples under natural irradiance and temperature conditions (Paerl et al., 1998). To estimate total C-production by phytoplankton for each ModMon sampling time point, the surface PP measurements for each station were multiplied by two to convert the daylight incubation period from 4 to 8 h (approximate length of daylight) and then multiplied by the surface volume (volume above the pycnocline) as defined for the salinity box model at each station and sampling date (Wetzel and Likens, 2000). The PP values as calculated for each station were then summed across the estuary for each ModMon date. Previous studies have estimated DOC production by phytoplankton as about 15–25% (averaged: 19%) of total C-production for coastal, eutrophic systems (Marañón et al., 2004). Therefore, the amount of DOC produced by phytoplankton was estimated as 15–25% of the total PP, with an averaged value of 19%, for the estuary. This represents a maximum amount of [DOC] produced by phytoplankton and does not capture net [DOC] from phytoplankton (i.e., [DOC] production by phytoplankton minus that removed by heterotrophic consumption).

All calculations, linear regression models, and statistical analyses were conducted in Matlab (2017b). Linear regression models were fitted using the Matlab *fitlm* function.

3. Results

3.1. Discrete discharge events

The time period used for this study encompassed a range of freshwater discharge conditions, spanning the 4th to 99th flow quantiles and included two hurricane-associated discharge events (Fig. 2, Table 1). The NRE was impacted by fringing effects from Hurricane Joaquin and an associated Nor'easter in September 2015, which resulted in elevated discharge from the NR and moderate wind conditions ($\sim 9\ m\ s^{-1}$ max. wind speed) over the NRE. In October 2016, the NRE and its watershed were directly impacted by Hurricane Matthew, which resulted in a historic 500-year flood event in the NR watershed (Musser et al., 2017). In addition to these two tropical storms, there were also several notable seasonal discharge events, including three sequential events in the winter of 2015–2016 and a spring discharge event in April 2016. All of these events were compared to a low-flow baseline period captured during summer 2015. We acknowledge the location of rainfall within the NR basin is important in altering the quantity and quality of DOC flushed from the watershed into the NRE following various discharge events. A discussion of this variability is included in the SI (Appendix 6).

3.2. DOM load

At the head of the estuary, [DOC] and a_{350} were positively and linearly correlated with discharge measured at Ft. Barnwell ($p < 0.001$ for both

parameters, with and without Hurricane Matthew) (Fig. 3a and b). DOC loads were positively and linearly correlated with a_{350} loads (Fig. 3c), indicating the DOC loaded into the estuary from the riverine end member was derived from terrestrial sources (Spencer et al., 2013). DOC and a_{350} loads were approximately twice as high immediately following Hurricane Matthew as for the other discharge events which had a large impact on the linear relationship between DOC and a_{350} loads and discharge.

3.3. Volume weighted DOM concentrations

Volume weighted [DOC] and a_{350} at each sampling time point closely followed the amount of freshwater in the estuary as indicated by its inverse relationship with salinity (Fig. 4; SI Fig. S13). The impacts of the wet 2015–2016 winter and Hurricane Matthew were obvious in both volume weighted DOM parameters ([DOC] and a_{350}) and volume-weighted salinity. In terms of volume-weighted salinity, there were similar values following the winter 2016 Pulse 3 event and Hurricane Matthew (~2 PSU), indicating the same volume of freshwater was flushed into the estuary during both of these events. The difference between these two events, however, was their duration: Pulses 1 through 3 occurred over several months while Hurricane Matthew's freshwater loading occurred within a span of days to weeks.

3.4. DOM estuarine processes

Unlike at the head of the estuary (Fig. 3a and b), [DOC] and a_{350} were not linearly correlated with estuarine inflow or outflow at station 160 (surface and bottom respectively) (Fig. 5a and b), indicating processes besides flow were dictating concentrations at the coastal end member. These processes could include biological (e.g., DOM consumption or production) or secondary sources of DOM within the estuary (e.g., wetlands; porewater resuspension).

3.4.1. Estuarine flow

For calculated estuarine flow at station 160, surface estuarine flow was generally out of the estuary with bottom estuarine flow into the estuary, following normal estuarine circulation (Geyer and MacCready, 2014) (Fig. 5c). Surface outflow at station 160 generally tracked riverine flow as measured at Ft. Barnwell, and DOC export was often driven by river flow (Figs. 3 and 5). However, under periods where there was significant stratification in the estuary, surface flow was largely driven by bottom water inflow from PS as would be predicted under normal estuarine circulation conditions (Geyer and MacCready, 2014). This large bottom water inflow from PS resulted in high surface water outflows at Station 160 that were not associated with especially high river flow, e.g. during the spring of 2016 and can be seen as the three time points associated with flow > 1000 $m^3 s^{-1}$ (Fig. 5a and b). Additionally, there were periods when the estuary exhibited reverse estuarine flow such that there was little to no flow in the surface waters at Station 160 and negative flows (i.e., flow out of the estuary) in the bottom water. Reverse estuarine flow has been documented in the lower NRE under NE winds (SI, Appendix 10) (Luettich et al., 2000).

3.5. Estimates of biological processes

Generally, the NRE was a sink for both a_{350} and DOC (Fig. 6a and b), with the highest sink terms in the weeks following tropical cyclone events (i.e., Joaquin, Matthew). Coinciding with this behavior, the estuary was a source of CO_2 to the atmosphere immediately following these events (~1 week) (Fig. 6c). PP was a significant source of total C, as both particulate OC (POC) and DOC, produced in the estuary (Fig. 6d) (Paerl et al., 1998). The magnitude of total C (POC + DOC) produced by PP was similar in magnitude to the DOC source & sink term for the NRE. However, assuming DOC production by phytoplankton is only 15–25% of total estuarine PP (Marañón et al., 2004), phytoplankton DOC production represents only a small fraction (< 10%) of the overall DOC source & sink term calculated for the NRE (Fig. 6d).

To assess tDOC removal in the estuary, the percent tDOC removed was calculated by dividing the DOC source & sink term as calculated for each time point by the river DOC load averaged across the flushing time at station 160 (Fig. 7; SI Appendix 7). Results plotted against averaged river DOC load demonstrate an exponential decrease. Values below 0%

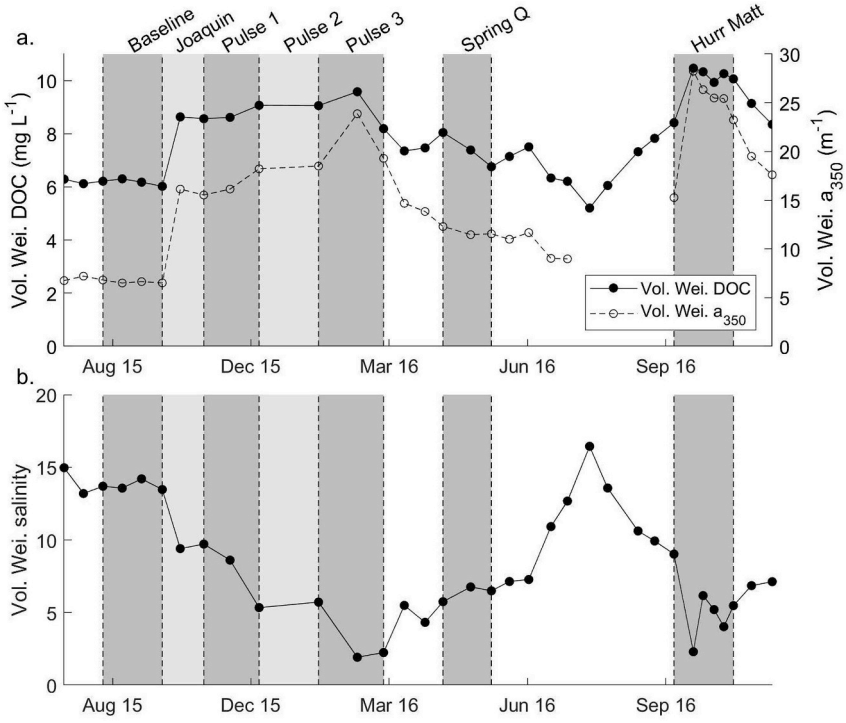

Figure 4. a. Volume weighted [DOC] (mg L^{-1}) plotted in the black circles and volume weighted a_{350} (m^{-1}) plotted in white circles. b. Volume weighted salinity. Dashed vertical lines indicate the boundaries of each of the 7 discrete discharge events.

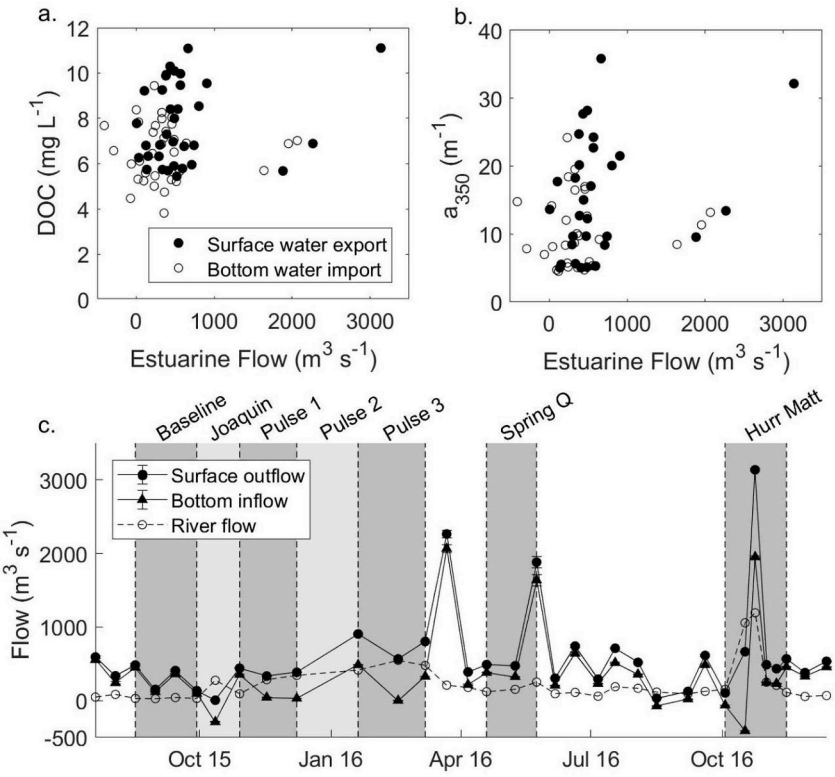

Figure 5. a. [DOC] (mg L^{-1}) and b. a_{350} (m^{-1}) plotted for station 160 versus estuarine flow. Black circles represent surface water at 160S and white circles represent bottom water at 180B. c. Estuarine flow (m^3 s^{-1}) as calculated for station 160. Surface outflow is plotted in the black circles, bottom inflow in the black triangles, and river flow as the white circles. Linear relationships were not statistically significant ($p > 0.1$).

indicate time points when DOC was 'produced' in the NRE (i.e., sediment resuspension; un-gaged tributaries; DOC production by PP) while values above 100% represent time points when the DOC pool in the NRE was dominated by mixing with DOC from PS, as further discussed below.

4. Discussion

It is well established that increasing freshwater discharge leads to increasing [DOC] and an increase in the terrestrial nature of DOC to downstream ecosystems, a paradigm that has previously been shown to apply in the NRE under both baseline and extreme discharge conditions (Dixon et al., 2014; Osburn et al., 2012; Paerl et al., 1998). Often lacking, though, are estimates of fluxes for individual estuaries based on observed properties of DOM and not inferred from modeled net ecosystem rates for large geographical regions (e.g., Herrmann et al., 2014; Najjar et al., 2018). Results from this study show that this paradigm applies when assessed for a single estuary, especially pertaining to DOC and a_{350} loading from the riverine end-member, where increasing riverine discharge resulted in a statistically significant, positive linear relationship between discharge and [DOC] and a_{350} both when including the high discharge value following Hurricane Matthew and when excluding this time point (Fig. 3a and b). These relationships led to increased DOM loads at the head of the estuary under elevated discharge conditions (Fig. 3c). Following Hurricane Matthew, there were indications of the 'dilution effect', where anomalously high discharge led to a decrease in [DOC] compared to what would be predicted by the positive, linear relationship between [DOC] and discharge under more normal flows ($Q < 750\,m^3\,s^{-1}$), as [DOC] was flushed from the watershed into the estuary.

The statistically significant, positive, linear relationship between DOC and a_{350} riverine loads indicate the DOC flushed into the estuary following these events is derived from terrestrial material stored in the NRE's watershed (Spencer et al., 2013). In the NRE, these terrestrial sources likely include flushing of terrestrial soils and freshwater wetlands, the latter of which are abundant between Ft. Barnwell and head of tides at station 0 (Rudolph, 2018). The extreme discharge following Hurricane Matthew, resulted in DOM loads that were as much as double those from any other discrete discharge event during this study (Fig. 3). The DOC and a_{350} loads computed following Hurricane Matthew demonstrated that the primary control on the NRE's C-cycle is likely caused by hydrologic connectivity of wetlands to the main river channel following EWEs, as was observed in the nearby Yadkin-PeeDee River basin (Majidzadeh et al., 2017).

4.1. DOM processes in the NRE

The goal of the project was to assess how the NRE responds to different discrete discharge events and establish under what discharge conditions the estuary might act as a sink for tDOC versus as a pipeline for export of un-altered tDOC to the downstream PS. To accomplish this, a DOC and a_{350} source & sink term was calculated for each ModMon date (Fig. 6a and b; Table 2). Overall, the NRE was a sink for DOC and a_{350} over the entire study period (~1.5 years), indicating the estuary was net heterotrophic; which has been observed for estuaries over annual time scales (Vlahos and Whitney, 2017). Annual-scale variation in river discharge has also been shown to affect net ecosystem metabolism in the nearby New River Estuary, NC, which varied between net autotrophy during a dry year, and net heterotrophy during a wet year (Crosswell et al., 2017).

In the present study, the box model occasionally indicated the NRE was a source of DOC and a_{350}, indicating that either DOM was produced internally or that secondary and tertiary sources of DOM were not accounted for with the box model (i.e., sedimentary and porewater resuspension; inputs from un-gaged tributaries and wetlands). While PP in the NRE is a significant source of total OC (TOC, as POC + DOC), the maximum amount of DOC possibly produced by PP, calculated as 19% of the total PP in the estuary (Marañón et al., 2004), is more than an order of magnitude less than DOC delivered to the estuary from the riverine end member (Fig. 6d). Therefore, we conclude that while DOC production by PP in the NRE represents a small source of DOC to the estuary ($1.61 \times 10^4 \pm 9.73 \times 10^2$ kg C d^{-1}, averaged), the magnitude of DOC produced by phytoplankton is often not large enough to account for the total amount of DOC produced in the estuary as estimated with the DOC source term. However, during the Spring Q period, the NRE was a weak source of DOC (8.08×10^3 kg C d^{-1}), despite relatively high riverine

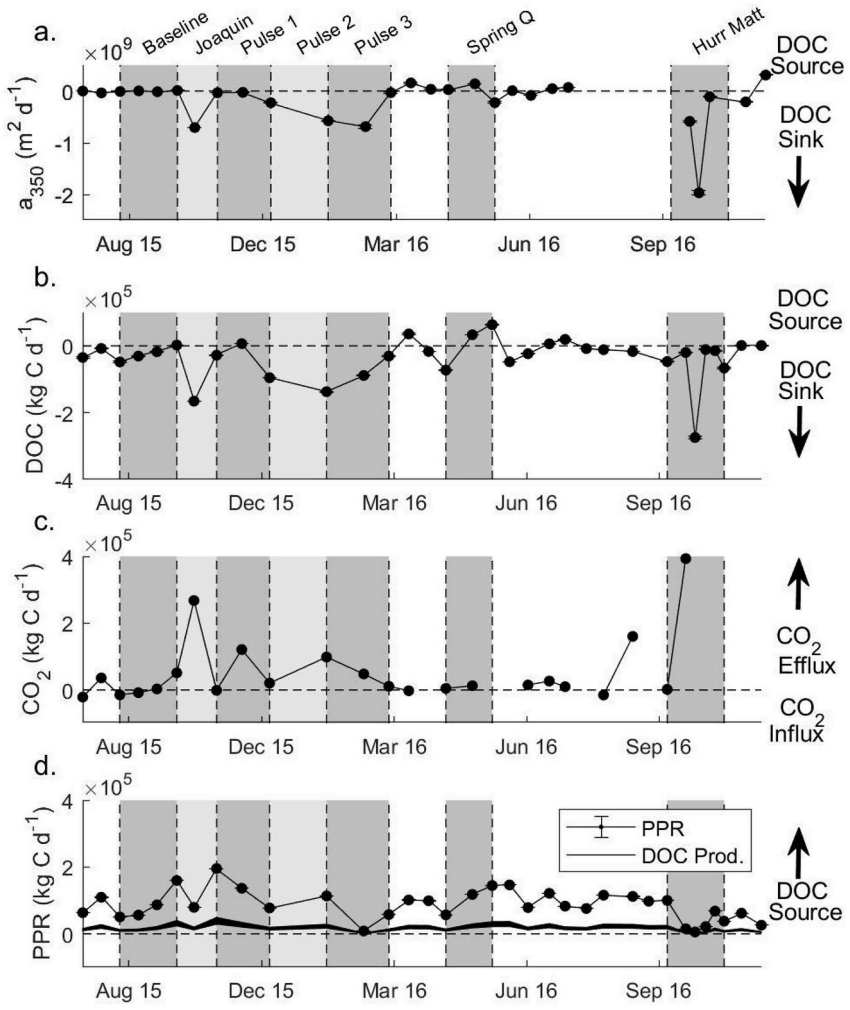

Fig. 6. Box model results showing a. a_{350} ($m^2\ d^{-1}$) and b. DOC (kg C d^{-1}) source & sink terms for each ModMon sampling date. Values represent internal estuarine a_{350} and DOC processing, respectively in excess of fluxes in and out of the system. c. water-air CO_2 flux (kg C d^{-1}). d. PPR (primary productivity, kg C d^{-1}) measured for the NRE plotted as black circles. DOC production by PP (estimated as 15–25% of total PP) is plotted in the shaded black area. In all graphs, the vertical dashed lines indicate bounds of the 7 discrete discharge events. The horizontal dashed line indicates 0.

DOC loading (1.18×10^5 kg C d^{-1}). During this time period, PP was estimated to produce 2.02×10^4 kg C d^{-1}; enough to account for the observed source term in the NRE, indicating PP may become a relatively important DOC source in this estuary during the spring season.

While it was beyond the scope of this study to specifically identify other sources of DOM to the estuary, we can speculate on potential mechanisms modulating DOM dynamics. The NRE is a relatively shallow estuary (average depth ~3.5 m) where resuspension events are common and well documented (Corbett, 2010). It is possible these resuspension events resulted in the release of previously deposited and stored C back to the water column (Crosswell et al., 2014; Luettich et al., 2000). Evidence from bottom water observations of DOM concentrations and properties from the NRE in 2010–2011 suggested higher [DOC] and more terrestrial-like DOM in bottom waters following

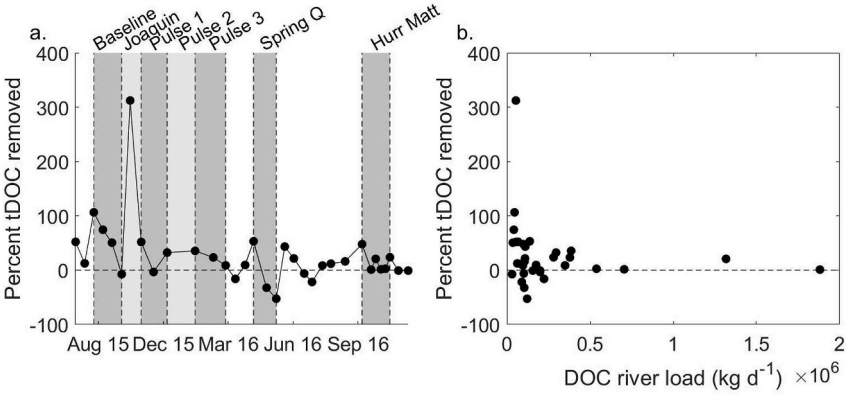

Figure 7. a. Percent tDOC removed plotted through time. b. Percent tDOC removed plotted against river DOC load (kg d^{-1}). The dashed line indicates 0%.

Table 2
Summary of C fluxes as averaged over each discrete discharge event including river DOC load as calculated for each ModMon sampling date, estuarine DOC export as calculated for station 160, the DOC source & sink term, PP production of DOC (assuming 19% of PP is produced as DOC), and CO_2 flux as reported in Van Dam et al. (2018). Confidence intervals are reported.

	River DOC load (kg C d^{-1})[a]	Estuarine DOC export (kg C d^{-1})[a]	PS DOC import (kg C d^{-1})[a]	DOC source & sink term (kg C d^{-1})[a]	PP DOC production (kg C d^{-1})**	CO_2 flux (kg C d^{-1})[b]
All	$1.81 \times 10^5 \pm 260$	$4.35 \times 10^5 \pm 6.02 \times 10^3$	$2.41 \times 10^5 \pm 6.42 \times 10^3$	$-2.64 \times 10^4 \pm 1.21 \times 10^4$	$1.61 \times 10^4 \pm 28$	$5.29 \times 10^4 \pm 1.00 \times 10^5$
Baseline	$1.74 \times 10^4 \pm 22$	$1.47 \times 10^5 \pm 5.46 \times 10^3$	$1.08 \times 10^5 \pm 5.46 \times 10^3$	$-2.35 \times 10^4 \pm 950$	$1.68 \times 10^4 \pm 32$	$7.77 \times 10^3 \pm 2.98 \times 10^4$
Joaquin	$1.11 \times 10^5 \pm 160$	$1.29 \times 10^5 \pm 3.58 \times 10^3$	$2.52 \times 10^4 \pm 3.58 \times 10^3$	$-6.37 \times 10^4 \pm 920$	$2.75 \times 10^4 \pm 51$	$1.06 \times 10^5 \pm 1.42 \times 10^5$
Pulse #1	$1.88 \times 10^5 \pm 230$	$3.05 \times 10^5 \pm 2.01 \times 10^3$	$7.43 \times 10^4 \pm 2.01 \times 10^3$	$-3.87 \times 10^4 \pm 800$	$2.59 \times 10^4 \pm 44$	$4.67 \times 10^4 \pm 6.52 \times 10^4$
Pulse #2	$2.58 \times 10^5 \pm 280$	$5.43 \times 10^5 \pm 2.47 \times 10^3$	$1.74 \times 10^5 \pm 2.47 \times 10^3$	$-1.16 \times 10^5 \pm 870$	$1.81 \times 10^4 \pm 43$	$5.95 \times 10^4 \pm 5.52 \times 10^4$
Pulse #3	$3.21 \times 10^5 \pm 350$	$6.28 \times 10^5 \pm 2.31 \times 10^3$	$1.99 \times 10^5 \pm 2.31 \times 10^3$	$-8.55 \times 10^4 \pm 900$	$1.14 \times 10^4 \pm 25$	$5.24 \times 10^4 \pm 4.40 \times 10^4$
Spring Q	$1.18 \times 10^5 \pm 150$	$5.16 \times 10^5 \pm 1.48 \times 10^4$	$3.96 \times 10^5 \pm 1.48 \times 10^4$	$8.08 \times 10^3 \pm 1.01 \times 10^3$	$2.02 \times 10^4 \pm 31$	$8.58 \times 10^3 \pm 5.80 \times 10^3$
Hurr Matt	$5.47 \times 10^5 \pm 900$	$1.02 \times 10^6 \pm 6.00 \times 10^3$	$3.94 \times 10^5 \pm 6.00 \times 10^3$	$-7.72 \times 10^4 \pm 2.05 \times 10^3$	$5.63 \times 10^3 \pm 10$	n.d.

[a] 95% confidence intervals calculated for each ModMon date using 1001 model runs, then averaged over the time period of interest. ** 95% confidence intervals calculated assuming PP ± 6% (SI, Appendix 2) then averaged over the time period of interest.
[b] Standard deviation of CO_2 flux calculated over each time period of interest. n.d. indicates no data.

wind-driven mixing events (Dixon et al., 2014). We approximated the DOC pool in sedimentary porewater to be about 1.66×10^5 kg C in the top 2.2 cm of sediment (SI, Appendix 8) which represents an additional source of DOC to the NRE, especially when riverine DOC loading is low and wind speeds are elevated. Preliminary experiments conducted during the summer of 2018 in the NRE indicate little [DOC] diffuses from the sediment porewater to the water column under calm conditions (Clerkin et al., unpublished).

Another source of DOC not accounted for in the calculated DOM source & sink term is un-gaged and un-characterized streams and tributaries lining the NRE. For example, the Trent River intersects the NRE between station 30 and 50 and contains dark, humic-rich water that has [DOC] and a_{350} about the same as the upper NRE, and which may represent an additional DOM source (Vähätalo et al., 2005). Additionally, there are several other smaller tributaries, pocosins, and wetlands along the NRE that could contribute to this un-accounted source of DOC. Generally, the NRE is a source of DOC under low flow conditions when contributions from the NR are relatively small in magnitude and DOC from these additional sources (i.e., PP, sediment porewater resuspension) may contribute relatively higher percentages of tDOC to the estuary.

A key result of this study is that the NRE is a tDOC sink in the weeks following elevated precipitation events and EWEs. This was especially evident 2 weeks following Joaquin and Hurricane Matthew. Previously, sustained (> 2 weeks) CO_2 efflux from estuaries following storm events has been attributed to *in situ* photochemical and microbial degradation of tDOC to CO_2 (Bianchi et al., 2013; Crosswell et al., 2014; Van Dam et al., 2018; Osburn et al., In Review). Approximately 2 weeks after Joaquin, estuarine-wide CO_2 efflux was estimated at 2.5×10^5 kg C d^{-1}, which was similar in magnitude to the $-1.66 \times 10^5 \pm 910$ kg C d^{-1} rate of DOC consumption (Fig. 8). Therefore, it appears that the conversion of tDOC to CO_2 by photochemical and microbial processes can explain approximately half (~66%) of the CO_2 efflux in the weeks following Joaquin. The remainder (~44%) of CO_2 emissions following Joaquin can then be attributed to a combination of CO_2 release from supersaturated riverine waters and sediment porewater resuspension. This is contrasted with large CO_2 fluxes observed immediately (0–7 days) following storm events that are largely driven by the delivery of poorly buffered river water, particularly in up-stream portions of the estuary heavily influenced by river inputs (Evans et al., 2013; Hunt et al., 2011; Van Dam et al., 2018).

Immediately following Hurricane Matthew (~7 days), measured CO_2 flux (3.93×10^5 kg C d^{-1}) was disproportionately large, relative to the DOC sink term ($-1.97 \times 10^4 \pm 1.30 \times 10^3$ kg C d^{-1}) (Fig. 6b and c, 8). The DOC sink term at this sampling time point was low under the short residence time, indicating the observed CO_2 flux likely was not due to oxidation of tDOC, as has been observed elsewhere (Crosswell et al., 2012; Evans et al., 2013; Hunt et al., 2011; Van Dam et al., 2018). Here, the NRE was dominated by outgassing of riverine CO_2 and the export of

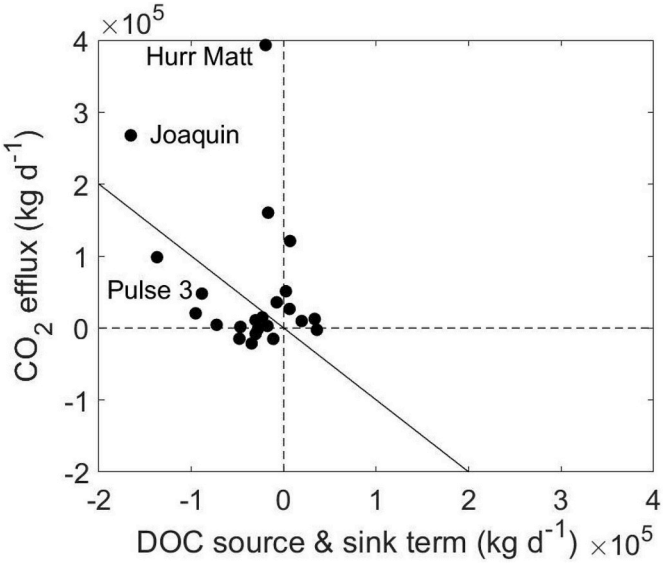

Fig. 8. CO_2 flux (kg C d^{-1}) from Van Dam et al. (2018) versus DOC source & sink term (kg C d^{-1}) for each sampling date. The 1:1 line is plotted (solid black line). The time points following Joaquin, Pulse 3, and Hurricane Matthew are identified.

TOC to downstream waters. In the weeks following Hurricane Matthew (~2 weeks post storm), as residence time increased, the NRE became a large sink for tDOC ($-2.74 \times 10^5 \pm 4.8 \times 10^3$ kg d^{-1}). While we only have direct estimates of CO_2 immediately following Matthew (~7 days), we hypothesize the positive CO_2 flux during this post-storm period would remain elevated in part due to microbial and photochemical oxidation of tDOC to DIC, as indicated by the large tDOC sink term (Crosswell et al., 2014). Additionally, PP measured in the weeks following Matthew was an order of magnitude lower (5.55×10^3 kg d^{-1}) than the average PP measured for the 1.5 year study (8.47×10^4 kg d^{-1}), indicating PP was not able to temper observed positive CO_2 fluxes in the weeks following Matthew. This is in contrast to the period following Joaquin, when a post-storm phytoplankton bloom caused the middle NRE to transition into a pCO_2 sink (Van Dam et al., 2018).

Therefore, we hypothesize that the NRE acted as a CO_2 source to the atmosphere operating under two separate, but related modes, following EWEs (Fig. 6b and c, 8). First, a ventilation mode occurred immediately (~1 week) following Hurricane Matthew (Van Dam et al., 2018). A low tDOC sink term combined with relatively poor carbonate system buffering, which together likely caused large and rapid ventilation of CO_2 to the atmosphere. Second, during the weeks (> 2 weeks) following Hurricane Matthew, we hypothesize the estuary switched to a reactor

Table 3
Estuarine C export (as DOC and TOC) estimated across systems located along the US east coast. Confidence intervals are reported when available.

Study system	Watershed area (km^2)[a]	C fraction[b]	Estuarine C export (kg C d^{-1})	Estuarine C export scaled to watershed (kg C d^{-1} km^{-2})	Reference
NRE	14,066				
All		DOC	$4.35 \times 10^5 \pm 6.02 \times 10^3$	30.9 ± 0.4	This study
Baseline		DOC	$1.47 \times 10^5 \pm 5.46 \times 10^3$	10.5 ± 0.4	This study
Joaquin		DOC	$1.29 \times 10^5 \pm 3.58 \times 10^3$	9.2 ± 0.3	This study
Pulse #1		DOC	$3.05 \times 10^5 \pm 2.01 \times 10^3$	21.7 ± 0.1	This study
Pulse #2		DOC	$5.43 \times 10^5 \pm 2.47 \times 10^3$	38.6 ± 0.2	This study
Pulse #3		DOC	$6.28 \times 10^5 \pm 2.31 \times 10^3$	44.6 ± 0.2	This study
Spring Q		DOC	$5.16 \times 10^5 \pm 1.48 \times 10^4$	36.7 ± 1.1	This study
Hurr Matt		DOC	$1.02 \times 10^6 \pm 6.00 \times 10^3$	72.5 ± 0.4	This study
South Atlantic Bight Estuaries	330,944	TOC	$5.48 \times 10^6 \pm 2.47 \times 10^6$	16.6 ± 7.5	Herrmann et al. (2014)
East Coast Estuaries	714,289	TOC	$9.32 \times 10^6 \pm 3.84 \times 10^6$	13.0 ± 5.4	Herrmann et al. (2014)
Long Island Sound, NY	42,373	DOC	$1.53 \times 10^5 \pm 1.75 \times 10^5$	3.6 ± 4.1	Vlahos and Whitney (2017)
Chesapeake Bay, VA	166,793	TOC	7.70×10^5	4.6	Kemp et al. (1997)
New River Estuary, NC	1177	TOC	1.29×10^4	11.0	Crosswell et al. (2017)

[a] Data obtained from Bricker et al. (2008).
[b] Indicates the fraction of C for which export values were calculated. DOC = dissolved organic carbon; TOC = total organic carbon (particulate OC (POC) + DOC).

mode in which large and positive CO_2 fluxes were sustained due to respiration of tDOC and DOC re-suspended from sedimentary pore waters (Crosswell et al., 2014; Dixon et al., 2014). Accordingly, in the weeks following Hurricane Matthew (> 2 weeks) we hypothesize the lower NRE became a sink for tDOC, in which its oxidation may have maintained this estuary as a source of CO_2 to the atmosphere. Thus, processes in the estuary may dramatically alter the terrestrial DOM pool before its eventual export to the coastal ocean in the weeks (2–3 weeks) following EWEs.

The DOC and CO_2 responses post Hurricane Matthew are markedly different from the responses following the Pulse 3 event (Fig. 8). Based on volume weighted salinity (Fig. 4), the same magnitude of freshwater was contained in the estuary following the Pulse 3 event as following Hurricane Matthew, however, the duration of these two events were different; the Pulse 3 event occurred over weeks to months while Matthew lasted days to weeks. This may have resulted in the mobilization of different DOC pools from the watershed, which could have affected the differential DOC and CO_2 responses following these two events (Rudolph, 2018; Osburn et al., In Review). Unlike the post-Matthew period, the NRE was a weak DOC sink ($-8.86 \times 10^4 \pm 700$ kg d^{-1}) and a weak CO_2 source (4.79×10^4 kg d^{-1}), falling below the 1:1 line. This indicates the CO_2 dynamics after Pulse 3 were largely controlled by tDOC oxidation (i.e., microbially or photochemically mediated) and positive CO_2 fluxes were potentially mitigated by increasing PP (Fig. 8) in contrast to the impact of Hurricane Matthew as discussed previously.

4.2. Pulse-shunt concept in estuarine ecosystems

The PSC suggests that under high river flow events (99th flow quantile), DOC pulsed from watersheds is shunted downstream (Raymond et al., 2016). Indeed, we observed the NRE acting as a source of tDOC to PS under high river flow events as has been shown previously (Osburn et al., 2016) (Fig. 6b). However, at mid-range river flow conditions the NRE acts as a weak sink for tDOC. Therefore, adapting the PSC as a paradigm for estuaries requires an assessment of what river discharge conditions the NRE acts as a sink for tDOC versus when the NRE acts as a source for tDOC export. The percentages of tDOC removed by the estuary at each sampling time point were calculated to quantify these modes and to adapt the PSC to estuaries (Fig. 7). Under certain river flow conditions (< 572 $m^3 s^{-1}$), model results showed that other sources of terrestrial-like DOC (i.e., sediment porewater diffusion and resuspension, un-gaged tributaries, adjacent tidal wetlands) were likely important. Additionally, under two river flow conditions (Q = 665 and 489 $m^3 s^{-1}$, respectively) when vertical stratification was strong, bottom water inflow at station 160 may have been high enough such that the dominant control on DOC dynamics in the NRE was mixing with PS water. Under these conditions, import of DOC from PS is much greater than import of tDOC from the riverine end member resulting in values of percent tDOC removed > 100%. This suggests two important possibilities: 1) despite the water residence time of months to more than a year in the PS (Paerl et al., 2018), its DOC is largely terrestrial in nature, and 2) tidal wetlands fringing the mouth of the NRE may contribute a large and unrealized amount of tDOC to this estuary under low flow conditions (Crosswell et al., 2014).

Immediately after extreme, 500-year flood events, like Hurricane Matthew (discharge > 1800 $m^3 s^{-1}$), only a small portion (~1%) of tDOC was removed in the NRE, indicating up to 99% of tDOC was exported directly to PS. This event resulted in an export of 1.86×10^6 kg C d^{-1} tDOC from the NRE to PS out of the 1.88×10^6 kg C d^{-1} tDOC for the total river load. However, under mid river flow conditions (340–1800 $m^3 s^{-1}$), between low- and high-flow, ~29% of tDOC was removed in the NRE (averaged for values between 0 and 100% tDOC removed excluding EWEs when river DOC load > 10×10^5 kg C d^{-1}; n = 21). Under these conditions, ~2.6×10^5 kg C d^{-1} of DOC was loaded into the NRE from the river end-member of which 1.8×10^5 kg C d^{-1} tDOC was exported to PS. These results indicate the 'pulse-mode' of the PSC holds true for river-dominated estuaries but only immediately following EWEs, like Hurricane Matthew (99th flow quantile), when nearly all tDOC was exported to adjacent coastal waters. Under all other ranges of flow conditions (4th to 89th flow quantile), as demonstrated in this multi-year study, the NRE acted as a weak to moderate sink for tDOC, processing an average of 29% tDOC which is close to the value estimated by Herrmann et al., 2014 for all US East Coast estuaries. The current study further indicates EWEs (> 99th flow quantile) can dramatically increase tDOC export from the NRE by an order of magnitude compared to moderate flow events, further demonstrating the role EWEs have on the C budget of coastal zones (Bianchi et al., 2013; Crosswell et al., 2014; Paerl et al., 2006).

Rainfall associated with Hurricane Matthew largely fell in the upper- and mid-NR watershed, meaning it took several weeks (> 2 weeks) for the NRE to receive the entire river pulse associated with Matthew (SI, Appendix 6). This resulted in elevated river DOC loading to the NRE even two weeks post-storm, which suggests that the 'pulse' from the NRE's watershed was gradual. Extensive flooding of riparian wetlands after Matthew's passage was observed and likely represented

an important source of the tDOC contained in the "pulse" (Rudolph, 2018). However, after this two-week period, the salinity of the estuary started to increase (Fig. 4b), indicating a return to normal estuarine circulation. We suspect that under these conditions, elevated tDOC loading from the NR was combined with import of previously exported, un-degraded tDOC from PS in the bottom water. Under these conditions, the estuary was a large sink of tDOC (Fig. 6b). Positive sea-to-air CO_2 fluxes were calculated for nearly two months post-Matthew (Osburn et al., In Review), similar to that observed following Joaquin and the Pulse 3 event. This result confirms our hypothesis that the large tDOC sink we have determined in this study resulted from tDOC that was photochemically and microbially-converted to CO_2.

Estuarine OC export, scaled to estuarine watershed area estimated for this study, is comparable to export values reported for other coastal ecosystems (Table 3). The NRE baseline, watershed normalized DOC export is in good agreement with watershed normalized TOC export calculated for other US East Coast estuaries as well as export values calculated for the South Atlantic Bight and US East Coast. The NRE baseline value is remarkably similar to the normalized TOC export calculated for the nearby New River Estuary (Crosswell et al., 2017). DOC is only a fraction of the TOC, which represents both DOC and POC and therefore, we would expect estimates of OC export from the NRE to increase if POC data were also included. Evidence in the NRE, however, suggests POC is only about 10% of the total TOC pool (Hounshell et al., unpublished). Unlike under baseline conditions, the NRE watershed normalized DOC export which includes elevated discharge events, is much greater than the baseline value and any of the other reported estuarine OC exports. This further indicates the large impact elevated discharge events have on altering the amount of OC exported from estuarine systems. Hurricane Matthew alone, exported up to 6 times more DOC than the TOC value estimated for all US East Coast estuaries (Herrmann et al., 2014). The paucity of EWE-related C export measurements likely means that regional C export from estuaries is under-estimated.

5. Conclusion

This study provided estimates of the major role EWEs play in modulating the coastal C-cycle and demonstrated that episodic events largely control lateral export of tDOC to coastal waters and flux of CO_2 from estuaries to the atmosphere. Evidence suggests the PSC paradigm for stream and river systems (Raymond et al., 2016) can be extended to estuaries, but only following extreme (99th flow quantile) events. Under all other flow conditions, as captured by this study, estuaries play an important role in modulating the terrestrial DOM pool prior to export to the coastal ocean, indicating the PSC as applied to estuaries should include a "process" component in order to have a holistic paradigm of the coastal C-cycle ranges from watershed to coastal ocean. Further, this study quantitatively linked tDOC oxidation in the estuary with observed CO_2 fluxes following several elevated precipitation events (Fig. 6b and c, 8); including Hurricane Matthew (Osburn et al., In Review), as shown for other events (Bianchi et al., 2013; Crosswell et al., 2014).

Results from this study indicate EWEs rapidly flush terrestrial DOM from the watershed into the estuary, which acts in concert with riverine CO_2 (Van Dam et al., 2018) to support very large CO_2 emissions. Soon after passage (~2 weeks) of these EWEs, the estuary switches back to a mode of tDOC processing. Due to the large tDOC inventories within the estuary following EWEs, large positive CO_2 fluxes are sustained due to photochemical and microbial processes which convert tDOC to CO_2 in the estuary. Therefore, EWEs will alter C-cycling in estuaries two ways: 1) increasing the amount of tDOC exported to downstream coastal systems and 2) enhancing efflux of riverine and estuarine CO_2 following these events. Both of these mechanisms should be incorporated into our understanding of how C-cycling will change in the future especially under predictions of increasing frequency and intensity of EWEs as predicted by climate change models (Bender et al., 2009; Janssen et al., 2016).

Declarations of interest

None.

Acknowledgments

We thank Betsy Abare, Jeremy Braddy, Thomas Clerkin, Lois Kelly, Karen Rossignol, and Randolph Sloup (UNC—CH IMS), as well as Stephen Richardson and Roxane Bowden (NCSU) for assistance with sample collection and analysis. Dr. Marc Alperin provided helpful advice and discussion concerning the salinity box model. We would also like to thank two anonymous reviewers for helpful comments which greatly improved this manuscript. The research was partially supported by NSF RAPID awards 1705872 (H.W.P.) and 1706009 (C.L.O.), North Carolina USGS-WRRI Student Fellowship (A.G.H.), and the North Carolina Dept. of Environmental Quality/National Fish and Wildlife Foundation Project ID #8020.16.053916 Neuse River Estuary Monitoring and Modeling Project, ModMon (H.W.P.).

Appendix A. Supplementary data

Supplementary data to this article can be found online at https://doi.org/10.1016/j.ecss.2019.01.020.

References

Alber, M., Sheldon, J.E., 1999. Use of a date-specific method to examine variability in the flushing times of Georgia estuaries. Estuar. Coast Shelf Sci. 49, 469–482.

Bauer, J.E., Cai, W., Raymond, P.A., Bianchi, T.S., Hopkinson, C.S., Regnier, P.A.G., 2013. The changing carbon cycle of the coastal ocean. Nature 504, 61–70. https://doi.org/10.1038/nature12857.

Bender, M.A., Knutson, T.R., Tuleya, R.E., Sirutis, J.J., Vecchi, G.A., Garner, S.T., Held, I.M., 2009. Modeled impact of anthropogenic atlantic hurricanes. Science 327, 454–458.

Bianchi, T.S., 2011. The role of terrestrially derived organic carbon in the coastal ocean: a changing paradigm and the priming effect. Proc. Natl. Acad. Sci. Unit. States Am. 108, 19473–19481. https://doi.org/10.1073/pnas.1017982108.

Bianchi, T.S., Garcia-Tigreros, F., Yvon-Lewis, S.A., Shields, M., Mills, H.J., Butman, D., Osburn, C., Raymond, P., Shank, G.C., Dimarco, S.F., Walker, N., Reese, B.K., Mullins-Perry, R., Quigg, A., Aiken, G.R., Grossman, E.L., 2013. Enhanced transfer of terrestrially derived carbon to the atmosphere in a flooding event. Geophys. Res. Lett. 40, 116–122. https://doi.org/10.1029/2012GL054145.

Bricker, S.B., Longstaff, B., Dennison, W., Jones, A., Boicourt, K., Wicks, C., Woerner, J., 2008. Effects of nutrient enrichment in the nation's estuaries: a decade of change. Harmful Algae 8, 21–32.

Christian, R.R., Boyer, J.N., Stanley, D.W., 1991. Multiyear distribution patterns of nutrients within the Neuse River estuary, North Carolina. Mar. Ecol. Prog. Ser. 71 (3), 259–274. https://doi.org/Doi 10.3354/Meps071259.

Corbett, D.R., 2010. Resuspension and estuarine nutrient cycling: insights from the Neuse River estuary. Biogeosciences 7, 3289–3300. https://doi.org/10.5194/bg-7-3289-2010.

Crosswell, J.R., Anderson, I.C., Stanhope, J.W., Van Dam, B.R., Brush, M.J., Ensign, S., Piehler, M.F., Mckee, B., Bost, M., Paerl, H.W., 2017. Carbon budget of a shallow, lagoonal estuary: transformations and source-sink dynamics along the river-estuary-ocean continuum. Limnol. Oceanogr. 62, S29–S45. https://doi.org/10.1002/lno.10631.

Crosswell, J.R., Wetz, M.S., Hales, B., Paerl, H.W., 2014. Extensive CO_2 emissions from shallow coastal waters during passage of Hurricane Irene (August 2011) over the Mid-Atlantic coast of the U.S.A. Limnol. Oceanogr. 59 (5), 1651–1665. https://doi.org/10.4319/lo.2014.59.5.1651.

Crosswell, J.R., Wetz, M.S., Hales, B., Paerl, H.W., 2012. Air-water CO_2 fluxes in the microtidal Neuse River Estuary, North Carolina. J. Geophys. Res. 117, 1–12. https://doi.org/10.1029/2012JC007925.

Del Giorgio, P.A., Pace, M.L., 2008. Relative independence of dissolved organic carbon transport and processing in a large temperate river: The Hudson River as both pipe and reactor. Limnol. Oceanogr. 53 (1), 185–197.

Dhillon, G.S., Inamdar, S., 2013. Extreme storms and changes in particulate and dissolved organic carbon in runoff: Entering uncharted waters? Geophys. Res. Lett. 40, 1322–1327. https://doi.org/10.1002/grl.50306.

Dixon, J.L., Osburn, C.L., Paerl, H.W., Peierls, B.L., 2014. Seasonal changes in estuarine dissolved organic matter due to variable flushing time and wind-driven mixing events. Estuar. Coast Shelf Sci. 151, 210–220. https://doi.org/10.1016/j.ecss.2014.10.013.

Evans, W., Hales, B., Strutton, P.G., 2013. pCO_2 distributions and air-water CO_2 fluxes in the Columbia River Estuary. Estuarine. Coast. Shelf Sci. 117, 260–272. https://doi.org/10.1016/j.ecss.2012.12.003.

Geyer, W.R., MacCready, P., 2014. The Estuarine Circulation. Annu. Rev. Fluid Mech. 46, 175–197. https://doi.org/10.1146/annurev-fluid-010313-141302.

Hagy, J.D., Boynton, W.R., Sanford, L.P., 2000. Estimation of net physical transport and hydraulic residence times for a coastal plain estuary using box models. Estuaries 23 (3), 328–340. https://doi.org/10.2307/1353325.

Hall, N.S., Paerl, H.W., Peierls, B.L., Whipple, A.C., Rossignol, K.L., 2013. Effects of climatic variability on phytoplankton community structure and bloom development in the eutrophic, microtidal, New River Estuary, North Carolina, USA. Estuar. Coast Shelf Sci. 117, 70–82. https://doi.org/10.1016/j.ecss.2012.10.004.

Herrmann, M., Najjar, R.G., Kemp, W.M., Alexander, R.B., Boyer, E.W., Cai, W., Griffith, P.C., Kroeger, K.D., McCallister, S.L., Smith, R.A., 2014. Net ecosystem production and organic carbon balance of U.S. East Coast estuaries: A synthesis approach. Glob. Biogeochem. Cycles 29, 96–111. https://doi.org/10.1002/2013GB004736.

Hirsch, R.M., De Cicco, L., 2015. User Guide to Exploration and Graphics for RivEr Trends (EGRET) and Data Retrieval: R Packages for Hydrologic Data (Version 2.0, February 2015), vol. 4 U.S. Geological Survey Techniques and Methods book chap A10, 93 pp.. https://doi.org/https://doi.org/10.3133/tm4A10.

Hunt, C.W., Salisbury, J.E., Vandemark, D., McGillis, W., 2011. Contrasting Carbon Dioxide Inputs and Exchange in Three Adjacent New England Estuaries. Estuar. Coasts 34, 68–77. https://doi.org/10.1007/s12237-010-9299-9.

Janssen, E., Sriver, R.L., Wuebbles, D.J., Kunkel, K.E., 2016. Seasonal and regional variations in extreme precipitation event frequency using CMIP5. Geophys. Res. Lett. 43, 5385–5393. https://doi.org/10.1002/2016GL069151.

Jiang, L., Cai, W., Wang, Y., 2008. A comparative study of carbon dioxide degassing in river- and marine-dominated estuaries. Limnol. Oceanogr. 53 (6), 2603–2615.

Kemp, W.M., Smith, E.M., Marvin-DiPasquale, M., Boynton, W.R., 1997. Organic carbon balance and net ecosystem metabolism in Chesapeake Bay. Mar. Ecol. Prog. Ser. 150, 229–248.

Luettich, R.A., Carr, S.D., Reynolds-Fleming, J. V, Fulcher, C.W., McNinch, J.E., 2002. Semi-diurnal seiching in a shallow, micro-tidal lagoonal estuary. Cont. Shelf Res. 22, 1669–1681.

Luettich, R.A., McNinch, J.E., Paerl, H.W., Peterson, C.H., Wells, J.T., Alperin, M.J., Martens, C.S., Pinckney, J.L., 2000. Neuse River Estuary Modeling and Monitoring Project Stage 1: Hydrography and Circulation, Water Column Nutrients and Productivity, Sedimentary Processes and Benthic-Pelagic Coupling, and Benthic Ecology. Technical Report No. 2000-325B. NC Water Research and Resources Institute, Raleigh, NC (Unpublished).

Majidzadeh, H., Uzun, H., Ruecker, A., Miller, D., Vernon, J., Zhang, H., Bao, S., Tsui, M.T.K., Karanfil, T., Chow, A.T., 2017. Extreme flooding mobilized dissolved organic matter from coastal forested wetlands. Biogeochemistry 136, 293–309. https://doi.org/10.1007/s10533-017-0394-x.

Marañón, E., Cermeñ0, P., Fernádez, E., Rodríguez, J., Zabala, L., 2004. Significance and mechanisms of photosynthetic production of dissolved organic carbon in a coastal eutrophic ecosystem. Limnol. Oceanogr. 49 (5), 1652–1666.

MATLAB and Statistics Toolbox Release. The MathWorks Inc, Natick, Massachusetts, United States.

Musser, J.W., Watson, K.M., Gotvald, A.M., 2017. Characterization of Peak Streamflows and Flood Inundation at Selected Areas in North Carolina Following Hurricane Matthew, October 2016 (Ver 1.1, June 2017). U.S. Geological Survey Open-File Report 2017-1047, p. 23. Unpublished. https://doi.org/10.3133/ofr20171047.

Najjar, R.G., Herrmann, M., Alexander, R., Boyer, E.W., Burdige, D.J., Butman, D., Cai, W., Canuel, E.A., Chen, R.F., Friedrichs, M.A.M., Feagin, R.A., Griffith, P.C., Hinson, A.L., Holmquist, J.R., Hu, X., Kemp, W.M., Kroeger, K.D., Mannino, A., Mccallister, S.L., McGillis, W.R., Mulholland, M.R., Pilskaln, C.H., Salisbury, J., Signorini, S.R., St-Laurent, P., Tian, H., Tzortziou, M., Vlahos, P., Wang, Z.A., Zimmerman, R.C., 2018. Carbon budget of tidal wetlands, estuaries, and shelf waters of Eastern North America. Glob. Biogeochem. Cycles 32, 1–28.

Osburn, C.L., Boyd, T.J., Montgomery, M.T., Bianchi, T.S., Coffin, R.B., Paerl, H.W., 2016. Optical Proxies for Terrestrial Dissolved Organic Matter in Estuaries and Coastal Waters. Frontiers in Marine Science 2 (127). https://doi.org/10.3389/fmars.2015.00127.

Osburn, C.L., Handsel, L.T., Mikan, M.P., Paerl, H.W., Montgomery, M.T., 2012. Fluorescence tracking of dissolved and particulate organic matter quality in a river-dominated estuary. Environ. Sci. Technol. 46, 8628–8636. https://doi.org/10.1021/es3007723.

Paerl, H., Pinckney, J., Fear, J., Peierls, B., 1998. Ecosystem responses to internal and watershed organic matter loading: consequences for hypoxia in the eutrophying Neuse River Estuary, North Carolina, USA. Mar. Ecol. Prog. Ser. 166, 17–25. https://doi.org/10.3354/meps166017.

Paerl, H.W., Bales, J.D., Ausley, L.W., Buzzelli, C.P., Crowder, L.B., Eby, L.A., Fear, J.M., Go, M., Peierls, B.L., Richardson, T.L., Ramus, J.S., 2001. Ecosystem impacts of three sequential hurricanes (Dennis, Floyd, and Irene) on the United States' largest lagoonal estuary, Pamlico Sound, NC. Proc. Natl. Acad. Sci. Unit. States Am. 98, 5655–5660. https://doi.org/10.1073/pnas.101097398.

Paerl, H.W., Crosswell, J.R., Dam, B. Van, Hall, N.S., Rossignol, K.L., Osburn, C.L., Hounshell, A.G., Sloup, R.S., Harding, L.W., 2018. Two decades of tropical cyclone impacts on North Carolina's estuarine carbon, nutrient and phytoplankton dynamics: implications for biogeochemical cycling and water quality in a stormier world. Biogeochemistry 141, 307–332. https://doi.org/10.1007/s10533-018-0438-x.

Paerl, H.W., Hall, N.S., Peierls, B.L., Rossignol, K.L., 2014. Evolving Paradigms and Challenges in Estuarine and Coastal Eutrophication Dynamics in a Culturally and Climatically Stressed World. Estuar. Coasts 37, 243–258. https://doi.org/10.1007/s12237-014-9773-x.

Paerl, H.W., Valdes, L.M., Joyner, A.R., Peierls, B.L., Piehler, M.F., Riggs, S.R., Christian, R.R., Eby, L.A., Crowder, L.B., Ramus, J.S., Clesceri, E.J., Buzzelli, C.P., Luettich, R.A., 2006. Ecological Response to Hurricane Events in the Pamlico Sound System, North Carolina, and Implications for Assessment and Management in a Regime of Increased Frequency. Estuar. Coasts 29, 1033–1045.

Peierls, B.L., Christian, R.R., Paerl, H.W., 2003. Water Quality and Phytoplankton as Indicators of Hurricane Impacts on a Large Estuarine Ecosystem. Estuaries 26 (5), 1329–1343. https://doi.org/10.1007/BF02803635.

Peierls, B.L., Hall, N.S., Paerl, H.W., 2012. Non-monotonic Responses of Phytoplankton Biomass Accumulation to Hydrologic Variability: A Comparison of Two Coastal Plain North Carolina Estuaries. Estuar. Coasts 35 (6), 1–17. https://doi.org/10.1007/s12237-012-9547-2.

Raymond, P.A., Saiers, J.E., 2010. Event controlled DOC export from forested watersheds. Biogeochemistry 100, 197–209. https://doi.org/10.1007/sl0533-010-9416-7.

Raymond, P.A., Saiers, J.E., Sobczak, W.V., 2016. Hydrological and biogeochemical controls on watershed dissolved organic matter transport: pulse-shunt concept. Ecology 97 (1), 5–16.

Rothenberger, M.B., Burkholder, J.M., Brownie, C., 2009. Long-Term Effects of Changing Land Use Practices on Surface Water Quality in a Coastal River and Lagoonal Estuary. Environ. Manag. 44, 505–523. https://doi.org/10.1007/s00267-009-9330-8.

Rudolph, J.C., 2018. Hurricane Matthew's Effect on Wetland Organic Matter Sources to the North Carolina Coastal Waters. Unpublished Thesis. North Carolina State University.

Sanderman, J., Lohse, K.A., Baldock, J.A., Amundson, R., 2009. Linking soils and streams: Sources and chemistry of dissolved organic matter in a small coastal watershed. Water Resour. Res. 45, 1–13. https://doi.org/10.1029/2008WR006977.

Spencer, R.G.M., Aiken, G.R., Dornblaser, M.M., Butler, K.D., Holmes, R.M., Fiske, G., Mann, P.J., Stubbins, A., 2013. Chromophoric dissolved organic matter export from U.S. Rivers. Geophys. Res. Lett. 40, 1575–1579. https://doi.org/10.1002/grl.50357.

Stackpoole, S.M., Stets, E.G., Clow, D.W., Burns, D.A., Aiken, G.R., Aulenbach, B.T., Creed, I.F., Hirsch, R.M., Laudon, H., Pellerin, B.A., Striegl, R.G., 2017. Spatial and temporal patterns of dissolved organic matter quantity and quality in the Mississippi River Basin, 1997–2013. Hydrol. Process. 31, 902–915. https://doi.org/10.1002/hyp.11072.

Stow, C., Borsuk, M.E., Stanley, D.W., 2001. Long-term Changes in Watershed Nutrient inputs and Riverine Exports in the Neuse River, North Carolina. Water Res. 35 (6), 1489–1499.

Vähätalo, A.V., Wetzel, R.G., Paerl, H.W., 2005. Light absorption by phytoplankton and chromophoric dissolved organic matter in the drainage basin and estuary of the Neuse River, North Carolina (U.S.A.). Freshw. Biol. 50, 477–493. https://doi.org/10.1111/j.1365-2427.2004.01335.x.

Van Dam, B.R., Crosswell, J.R., Anderson, I.C., Paerl, H.W., 2018. Watershed-scale drivers of air-water CO2 exchanges in two lagoonal North Carolina (USA) estuaries. J. Geophys. Res.: Biogeosciences 123, 271–287.

Vlahos, P., Whitney, M.M., 2017. Organic carbon patterns and budgets in the Long Island Sound estuary. Limnol. Oceanogr. 62, S46–S57. https://doi.org/10.1002/lno.10638.

Wetzel, R.G., Likens, G.E., 2000. Primary productivity of phytoplankton. In: Limnological Analyses. Springer, New York, pp. 219–240.

Yoon, B., Raymond, P.A., 2012. Dissolved organic matter export from a forested watershed during Hurricane Irene. Geophys. Res. Lett. 39, 1–6. https://doi.org/10.1029/2012GL052785.